# REPRODUCIBILITY OF HEAT TRANSFER TESTS IN A 5X5 BUNDLE GEOMETRY

By

G. Cubizolles<sup>1</sup>, P. Clement<sup>1</sup> and D. Groeneveld<sup>2</sup>,

<sup>1</sup>Commissariat à L'Energie Atomique et aux Energies Alternatives (CEA), Grenoble, France;

<sup>2</sup>University of Ottawa, Canada and AECL, Chalk River, Canada

## **ABSTRACT**

This paper describes the repeatability and reliability of bundle heat transfer data obtained in a 5X5 PWR-type bundle subassembly operating at PWR conditions of interest. The 5X5 fuel bundle simulator, installed in the OMEGA-2 loop, is equipped with simple support grids, designed to have a low impact on the flow and heat transfer. The nine central heaters were equipped with the novel sliding thermocouple technique, capable of measuring the detailed axial and circumferential temperature distributions during single-phase and boiling heat transfer tests.

In order to obtain highly accurate bundle heat transfer measurements, appropriate experimental procedures and in-situ calibrations of all essential instrumentation were employed. This includes (i) the employment of calibrated reference fluid temperature measurement devices, (ii) in-situ calibrations of fluid and heater-sheath thermocouples, (iii) calibration of heater wall thickness based on in-situ measurements, and (iv) selection of data that satisfy strict acceptance criteria.

After applying these corrections and data screening criteria, the measurement accuracy and repeatability was assessed. This was done by means of three different tests:

- <u>Single Phase Heat Transfer</u>: The repeatability of heat transfer were assessed by comparing the measurements of two separate 5X5 bundles against the predictions from a Dittus-Boelter-type heat transfer correlation which provided very similar results. Also the single-phase heat transfer repeatability was assessed by performing several repeat runs and comparing results obtained on heaters in symmetric locations. Excellent repeatability was noted and the results for symmetric angular locations are almost identical.
- <u>Boiling Tests:</u> During the boiling heat transfer tests excellent repeatability and symmetry was observed. The saturation temperature (corresponding to the measured outlet temperature) was found to be in very good agreement with (i) the outlet temperature measured by the platinum resistance temperature detector (RTD) (average difference 0.1 K, range 0 to 0.2 K) and (ii) the average of the 36 subchannel outlet-coolant temperature measurements (average difference 0.1 K, range +0.5 to -0.6 K).
- Onset of Nucleate Boiling (ONB) Tests: for all tests performed at a constant pressure, heat flux and mass velocity, the ONB for the same symmetric position occurs at the same thermodynamic quality irrespective of location of the nearest grid. Repeatability was again excellent

The results demonstrate the capability of the OMEGA-2 loop in obtaining highly accurate and repeatable single-phase and boiling heat transfer measurements in PWR-type subassemblies.

## 1. INTRODUCTION

The intent of this paper is to examine the repeatability and consistency of heat transfer tests performed in large scale bundle geometries. There is a common misconception that, because of the complexity of bundle geometry, with its frequent grids and possibility of bundle deformation

due to Laplace forces and differential expansion etc., bundle heat transfer tests are significantly less accurate then tube-based heat transfer tests.

The tests described in this paper were performed in the OMEGA-2 test facility of CEA in Grenoble France on a 5X5 bundle geometry, commonly used for PWR fuel-bundle simulations. The test conditions are typical of those encountered in PWR bundles. No unusual equipment was used except for the sliding thermocouple technique which has been described in detail in previous papers (Cubizolles et. al., [1]; Schenk and Groeneveld, [6]) and in more general terms in Section 2. The accuracy of the results was found comparable to measurements in simple geometries.

The main sources of uncertainty in bundle heat transfer experiments are:

- bundle geometry uncertainty: the impact of Laplace forces in directly heated tubes that attract adjacent parallel heater tubes when a large DC current passes through the tube sheaths,
- heater-sheath thickness variation: in previous experiments, variation in circumferential
  heat flux due to wall thickness variations are ignored because of (i) the lack of
  circumferential temperature distributions, required to estimate and correct for wall
  thickness variations and (ii) the difficulty to accurately measure the wall thickness
  variations without a destructive testing,
- uncertainty in flow conditions: flow, pressure, coolant temperature and power measurements.
- uncertainty in sheath temperature measurements including the distribution in sheath temperature, and
- presence of outliers.

This paper describes how the impact of these sources of errors was minimized and quantifies the accuracy and repeatability of the heat transfer measurements.

## 2. DESCRIPTION OF EXPERIMENTAL EQUIPMENT

## 2.1 OMEGA-2 Test Facility

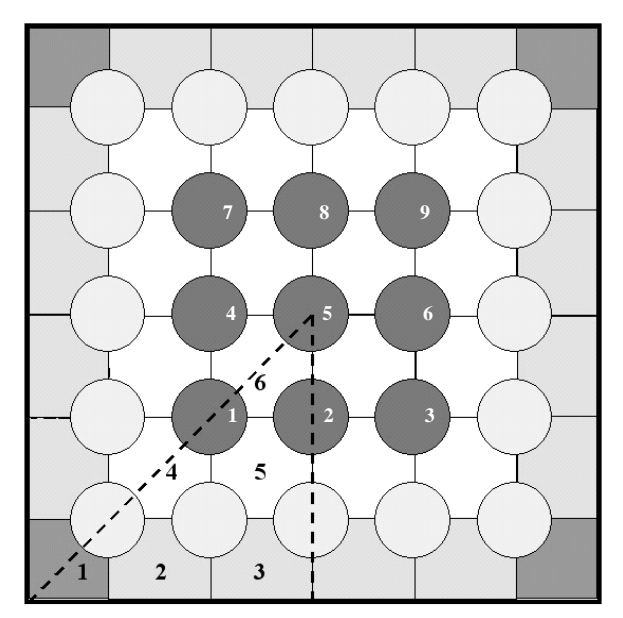
The recently upgraded OMEGA-2 test facility at CEA Grenoble is a high-pressure water loop capable of simulating a 5X5 rod PWR bundle subassembly at PWR conditions of interest. The maximum pressure of the loop is 17 MPa. A 10 MW power supply simulates nuclear heating by direct Joule heating of the 25 heater tubes (maximum current 40 000 Amp). Details of the loop have been described by Cubizolles et al., [1].

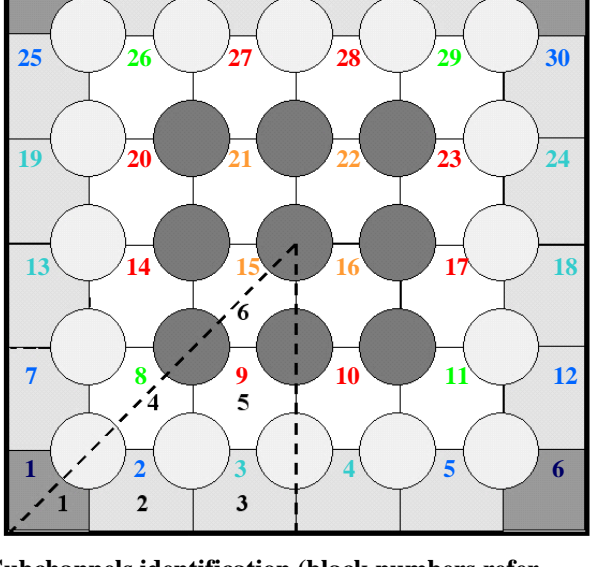
## 2.2 Test Section Geometry

A ceramic liner provides electrical insulation between the 5X5 fuel simulator and the pressure tube, and acts as a flow channel for the coolant. The 25 heater tubes of the fuel bundle simulator have an OD of 9.5 mm, a heated length of 3.658 m, a constant wall thickness (thus providing a uniform axial power profile), and are arranged on a square array with a pitch of 12.6 mm. The bundle is designed such that the heat flux ratio between the 9 central and 16 peripheral tubes is 1.3. This ratio was achieved by having different inside diameters (7.7 and 8.15 mm respectively for the central and peripheral tubes). Figure 1 shows the bundle cross-section with the numbering of the instrumented central support rods and subchannels. This figure also shows the subchannels types identified for the bottom left quadrant only.

Joule heating of the heater tubes induces electromagnetic forces also called Laplace forces which can result in unacceptable heater bow. The deformation of heater tubes is a function of electrical heating current and distance between grids. To maintain the rod spacing of 3.1 mm

along the 3.66 m heated length under actual heating conditions of 900 kW/m² requires the presence of a grid (either a simple support grid (SSG) or a mixing vane grid (MVG)), every 279 mm, as was shown in [7]. The SSG presence midway between adjacent MVGs reduces the bow from about 300  $\mu$ m to 30  $\mu$ m (i.e. comparable to the rod diameter uncertainty  $\pm$  20  $\mu$ m To minimize the SSG impact on the heat transfer and coolant flow, the length of the SSG is only 8 mm and the thickness is reduced to 0.2 mm.





32

31

33

34

35

36

**Instrumented heater rods identification** 

Subchannels identification (black numbers refer to subchannel type)

Figure 1: 5X5 Bundle Cross Section.

#### 2.3 Instrumentation

Flow conditions: The pressure is measured twice at the inlet and the outlet of the test section by pressure transducers having a range of 0 - 20 MPa and a measurement accuracy of 100 kPa. The accuracy of the pressure drop measurement (using DP cells) across the test section is 0.5% of full scale. Several nozzle-type flow meters and turbine flow meters are employed in the OMEGA-2 loop, covering many ranges of flow and providing redundancy measurements. The mass flow rate ranged between 7 to 12 kg/s for the 5X5 bundle test section and was measured with an accuracy of 1%. The test section power and the power supplied to each the heater rods are calculated from voltage and current measurements at the test section terminals and from the heater rod resistance measurements – the uncertainty in power measurements is less than 0.1%.

Coolant Temperatures: The average coolant temperature is measured at the inlet and outlet of the test section using two platinum resistance temperature detectors (RTDs). The probes are calibrated at twelve reference points where the temperature level is controlled at  $\pm$  0.05 K between 0 and 350°C. The temperature measurement accuracy is 0.2 K. The coolant temperature distribution at the end of the heated length is measured at the centre of each of the 36 subchannels, by type N thermocouples (Nisil-Nicrosil). These thermocouples are insulated (resistance junction-to-sheath: >1M $\Omega$ /250V) and have an Inconel 600 sheath with an OD of 1 mm. The thermocouples are supported by a specially-designed thermocouple-support grid located just downstream of the end of the heated length (EOHL).

<u>Wall temperature</u>: To properly characterize the heat transfer in a bundle geometry equipped with grids, one needs to know the surface temperature distribution. All previous PWR heat transfer tests used fixed thermocouples located inside the heater rods. The OMEGA-2 loop uses the novel sliding thermocouple technique, used previously in CANDU bundle heat transfer tests

(Schenk and Groeneveld, [6]; Leung et al., [5]). The present approach consists of using sliding temperature sensors, equipped with thermocouples, that can measure the complete axial and circumferential temperature distribution at the inside surface of the nine central heater rods (3X3) of the test bundle. The temperature at the heat transfer surface can be obtained from the measured temperature distribution after applying the appropriate heat conduction equations.

The sliding thermocouple assemblies (also called "sliders" or "probes") for the inner rods were made to specification after a strict qualification process. The sliders were equipped with four type N thermocouples distributed over two thermocouple ceramic carriers spaced axially by 0.558 m. Good thermal contact between sliding thermocouple and heater rod inner surface is obtained by using the thermocouple sheath as a spring as can be seen in Figure 2. The thermocouple junctions were ungrounded, i.e. they were electrically insulated from the thermocouple's Inconel 600 sheath. This sheath was in direct contact with the heated wall but was electrically insulated from the probe main body by the ceramic thermocouple carrier.

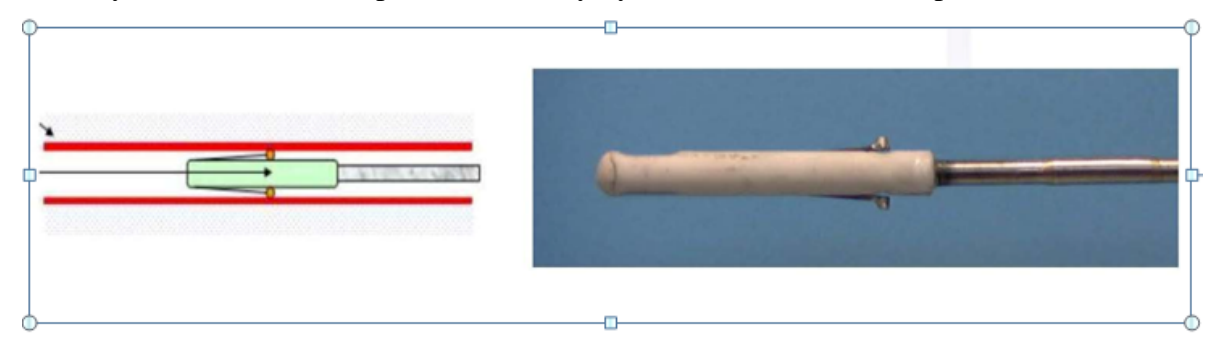


Figure 2: Sliding Thermocouple Details.

The thermocouple slider movement is controlled by a slider displacement system. Two motors move the slider trolley axially or rotate the sliders by means of a transmission belt. The displacement system controls the thermocouple tip position by counting the revolutions of the motors. To determine the measurement position, each slider probe is linked to a precision potentiometer (linearity better than  $\pm$  0.15% for angular displacements and better than  $\pm$  0.10% for axial displacements). The angular measurement accuracy is  $\pm$  1° while the axial-position measurement accuracy (after applying corrections to account for thermal expansion of (i) copper upper extension of the heater rod, (ii) Inconel 600 heater tube, (iii) inserted SS 316L slider probe guide tube) is  $\pm$  1 mm. More details are given by Cubizolles et al., [1].

#### 3. EXPERIMENT

#### 3.1 Test Conditions

The experiments covered typical PWR-type conditions i.e. G:  $3000-4600 \text{ kg/m}^2/\text{s}$ , P: 100-155 bar, q:  $570 \text{ to } 1400 \text{ kW/m}^2$  and Ti: 185 - 305 °C. Four types of tests were completed during the test campaign:

## • Thermocouple calibration tests at adiabatic conditions:

The N-types thermocouples were used to measure sheath temperatures. To reduce the thermocouple uncertainties from the usual specified values, the thermocouples were calibrated in situ against reference temperatures, provided by the platinum RTDs at the inlet and outlet. The in situ calibration tests were performed at adiabatic conditions and high flows, where the flow is virtually isothermal.

# • Single Phase Heat Transfer tests:

This part of the test campaign provides the internal wall temperatures and the coolant temperatures at the centre of the sub-channels at the end of the heated length. These values

are necessary for the assessment and/or development of bundle/subchannel/local heat transfer correlations.

# • <u>Saturated Boiling tests</u>:

During the boiling tests, detailed inner wall temperature distributions were measured for all instrumented rods. To ensure that boiling occurred, these tests were performed with positive qualities in the test section over the thermocouple probe measurement trajectory (0 to -1.1 m from EOHL). The measured inner wall boiling temperatures were subsequently used to (i) obtain the circumferential variation in wall thickness (Section 4.4) and (ii) check repeatability.

## • Onset of Nucleate Boiling tests:

These tests are performed to accurately determine the boiling boundaries on the outside heater surface, based on the inner rod temperature measurement. The occurrence of ONB is characterized by a change from a linear axial wall temperature gradient (typical of single phase heat transfer) to a nearly flat wall temperature profile (typical of nucleate boiling).

## 3.2 Test Procedure

The test procedures for the single phase, the ONB and the boiling tests are very similar: After establishing the desired flow conditions and coolant temperatures, all flow conditions, subchannel temperatures and wall temperatures are measured for each position of the thermocouple sliders. The repositioning of the slider is done first by rotation and subsequently by axial movement. The measurements start with the slider at the most downstream position (z = 0.0 m, EOHL), and is completed when the slider reaches its most upstream position (i.e. when it is completely inserted into the heater). The most upstream axial measurement position is about -1.2 m for all tests while the axial displacement is in steps of 20 mm. The circumferential displacement is in steps of  $20^{\circ}$ .

The temperature data acquisition begins after repositioning the slider and allowing the probe temperatures to stabilize. The stabilization period varies and depends on whether the new location is the first of a circumferential profile (about 30s) or a subsequent point (about 10s). Then the data acquisition collects and averages a number of scans (usually about 10) for each slider thermocouple over a period of 2 seconds. After the averaging process, the measured values are converted into engineering units after applying the appropriate calibrations. Note that the mass velocity and the position of the sensors are corrected for thermal expansion of the test section and slider guide tube. During a typical test  $10(\# \text{ of scans}) \times 9(\# \text{ of rods}) \times 18(\# \text{ of angular positions}) \times 60(\# \text{ of axial positions}) = 97,200 \text{ surface temperature measurements were obtained.}$  After averaging, up to 9720 measurements per run were used in the subsequent data analysis; in total 15 single phase runs and 21 ONB / boiling runs were completed.

## 4. PROCEDURES FOR ENHANCING MEASUREMENT ACCURACY

#### **4.1 Heat Loss Calibration**

Heat loss calibrations were first performed for adiabatic tests for a 125-350 °C range of coolant temperatures. A best-fit line for heat loss as a function of coolant temperature was derived – only 0.6 to 2.4% of the power (average 1.1%) was lost due to heat loss or is due to uncertainties in flow (Q), power (W), inlet and outlet temperatures. Applying the corrections for heat loss resulted in a final heat balances (= W - Q×(Ho-Hi)) having only a  $\pm$  0.3% variation. This final heat balance agreement is excellent and provides further proof of the high quality of the measured flow and coolant parameters.

#### **4.2 Data Selection**

To ensure the highest reliability of the data requires a strict data filtering process that will eliminate measurements at unstable conditions and measurements from thermocouples having a questionable reliability. The following data acceptance criteria were applied: (i) heat balance < 1% (heat balances were evaluated for all single phase heat transfer and subcooled boiling tests), (ii) flow and power variations during the data averaging process < 1%, (iii) pressure variations < 0.5 bar, and (iv) coolant temperature variations < 0.2 K. More that 90% of the data passed the acceptance criteria and were subsequently used in the data analysis.

Measurements performed near the end of heated length (axial location z > -50 mm) were also eliminated because here the inner wall temperature may be affected by heat conduction to the copper extensions.

# 4.3 Thermocouple Calibration

Calibration tests precede the heat transfer tests and consist of the following steps: (i) establish isothermal conditions in the loop at various temperature levels (covering the temperature range of interest), (ii) for each temperature, obtain a map of measured wall temperatures covering the full axial and circumferential trajectory to be covered during the tests, and (iii) construct a regression line for each thermocouple by comparing the measured temperatures for each thermocouple (obtained from the standard calibration curve [8, 9] for type N thermocouples) to the true temperature provided by the platinum RTDs. A new calibration was performed each time a change in wall temperature measurement system occurs i.e. a sliding probe change or repair.

For the sliding probe thermocouples, the true temperature is interpolated as a function of axial location assuming temperature decreases (due to heat losses) linearly from inlet to outlet. The thermocouple calibration results show that:

- root mean square (RMS) deviation from the regression lines is less than 0.2 K for the sliding probe thermocouples and less than 0.15 K for fluid thermocouples,
- the maximum calibration error is less than 0.4 K for more than 99% of the data from wall and fluid thermocouples, except for two wall thermocouples for which the calibration error is less than 0.4 K for 89 % of the data,
- during the calibration process the wall temperature measurements showed an axial variation of less than 0.3 K.

#### **4.4 Wall Thickness Correction**

A sinusoidal temperature distribution around the periphery of the heater rods was observed during the boiling tests, e.g. see Figure 3. The sinusoidal temperature distribution strongly suggests a variation in wall thickness due to an eccentric ID with respect to the OD. A methodology was subsequently derived to account for the wall thickness variation in the wall-temperature-drop calculation process based on the heat conduction equation and assuming a flat circumferential outside-wall-temperature profile during nucleate boiling (Cubizolles et al, [2]). Based on this methodology, heater-rod thickness maps were constructed for each heater rod as a function of axial and angular location. As expected from the manufacturing process the impact of axial location on the wall thickness is not significant but the calculated circumferential wall thickness profiles indicated an eccentric ID with respect to the OD. Subsequent ultrasonic wall thickness measurements confirmed the calculated wall thickness profiles and eccentricity. The corrected wall thickness was used to more accurately calculate the local heat flux and outside wall temperatures for the single phase tests.

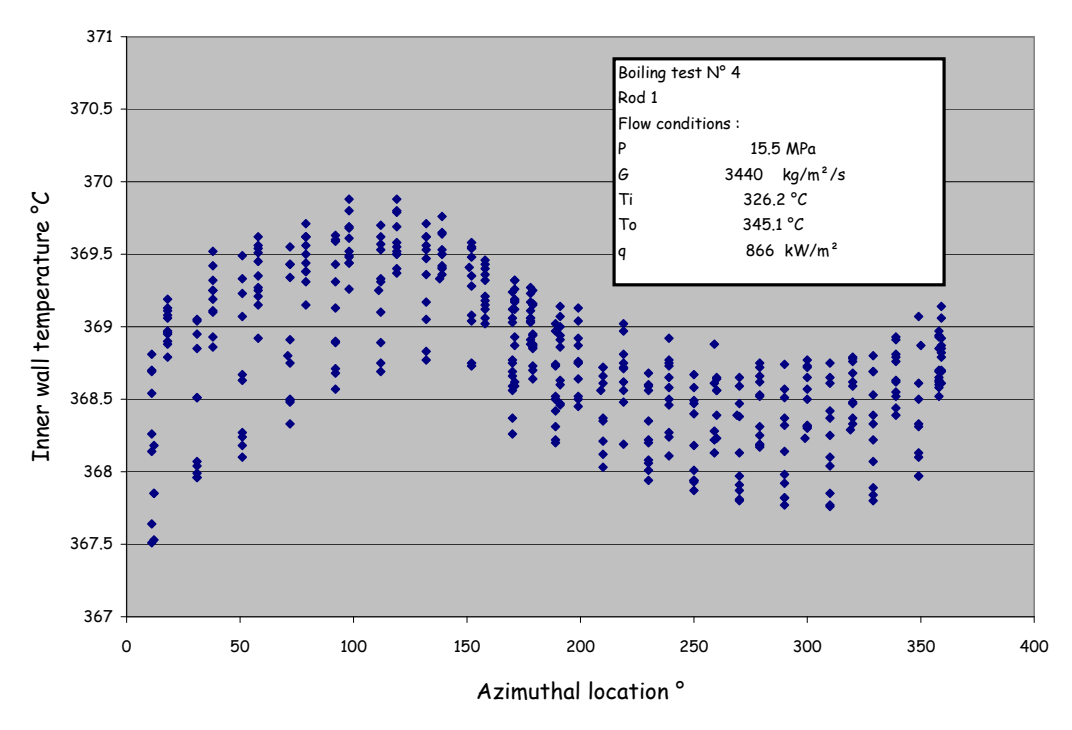


Figure 3: Circumferential Temperature Profiles for Boiling Test N°4 Rod No. 1.

Note that in PWR experiments performed elsewhere, this correction is ignored because of the lack of circumferential temperature distributions, required to correct for wall thickness and heat flux variations. Only because of the use of the sliding thermocouple technology were we able to correct for these systematic variations in heat flux and wall temperature drop.

Figure 4 (figure on left) shows a typical axial temperature gradient measured on Rod No. 1 during boiling test 4. The average wall temperature gradient is slightly negative – this is attributed to the saturation pressure gradient along the heated length. Although the scatter in measured inside wall temperature is significant and is due to the non-uniform circumferential wall thickness variation as discussed in Section 4.4 (all temperatures measured at 20° angular intervals are shown), after the correction for non-uniform wall thickness has been applied this scatter is no longer observable on the outside wall temperature vs. axial location plot (Figure 4, figure on right). Thus implementing the wall thickness correction procedure improves the accuracy of heat transfer coefficient extracted from the experimental data significantly.

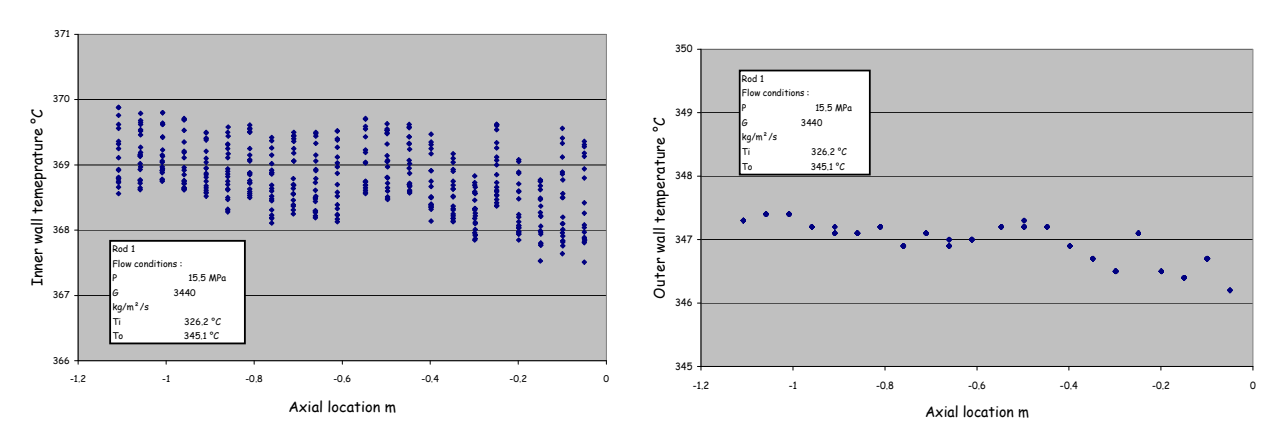


Figure 4: Axial Variation in Wall Temperature During Boiling Test #4.

#### 5. REPRODUCIBILITY OF SINGLE PHASE HEAT TRANSFER RESULTS

One of the main objectives of the current tests is to establish a reference data bank for singlephase heat transfer in a rod bundle at PWR conditions, as a comparison basis for tests on bundles equipped with mixing vanes.

A check on single-phase data repeatability and symmetry is illustrated in Figure 5 for the central rod, Run 4 and its repeat runs. To account for differences in inlet temperature, the outer wall temperature is plotted against the thermodynamic quality. For all runs and all angles, the axial variation in quarter-averaged outer-wall temperature can be presented by a simple linear regression function. The RMS deviation is 0.8 K; some of this variation is due to variation in flow conditions between runs and variation in circumferential heat flux. Visual inspection of Figure 5 suggests that repeatability (from run to run) is excellent and the results for symmetric angular locations are almost the same. A similar observation was made for the side rods and corner rods of the 3X3 array of instrumented inner rods. The overall conclusion is that the single phase results demonstrate excellent repeatability and symmetry.

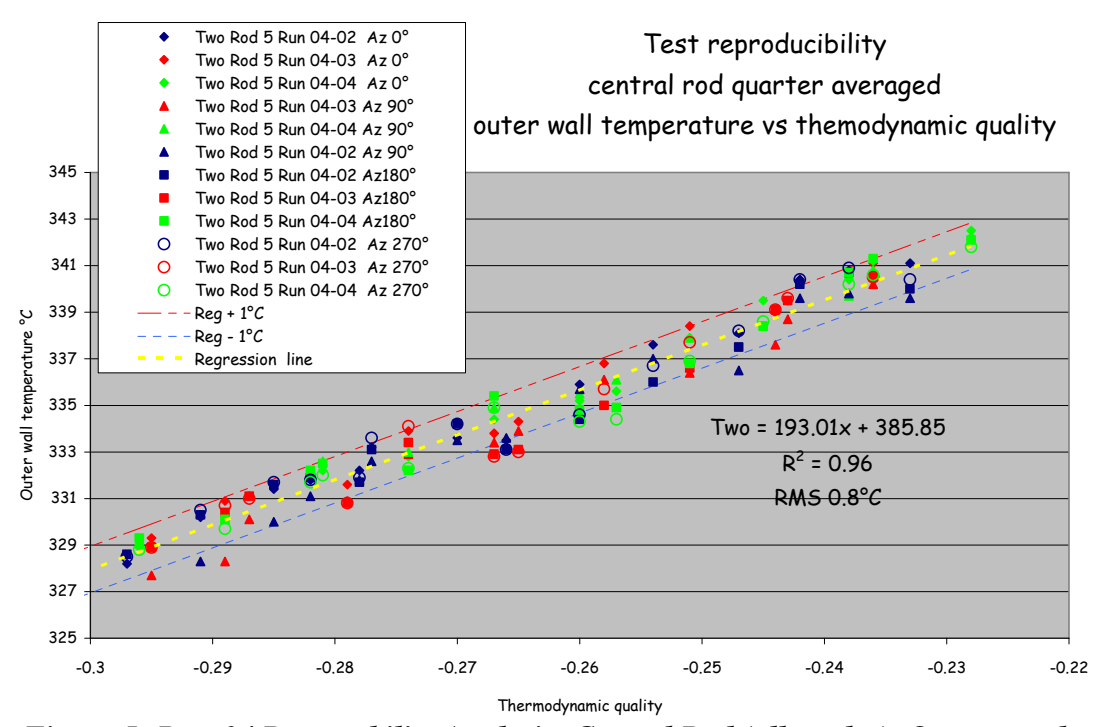


Figure 5: Run 04 Repeatability Analysis: Central Rod (all angles), Quarter-rod-averaged Outer Wall Temperature vs. Quality,  $G=3500 \text{ kg/(m}^2\text{s})$ , P=15.5 MPa,  $q=900 \text{ kW/m}^2$ .

To check the consistency of the collected data, the "experimental heat transfer coefficient" was first compared to predictions from the Dittus-Boelter [3] heat transfer correlation,

 $Nu = 0.023 \,\mathrm{Re}^{0.8} \,\mathrm{Pr}^{1/3}$ 

<sup>&</sup>lt;sup>1</sup> The "experimental" heat transfer coefficient  $h = q/(T_{wo} - T_f)$ ,  $T_{wo}$  is outer wall temperature, obtained using the measured inner wall temperature based on the wall thickness correction methodology, and  $T_f$  (Az, Z) is the local coolant temperature, calculated from coolant temperature measured at the end of heated length in the centre of each subchannel assuming (i) axial linear variation from test section inlet to the end of heated length, and (ii) linear transverse fluid temperature variation by quadrant (-45° to 45°, 45 to 135°, 135 to 225° and 225 to 315°) between adjacent subchannels.

where the fluid properties are evaluated at the film temperature  $T_{film} = (T_{wo} + T_f)/2$ ,  $T_f$  is the local fluid temperature  $T_{film} = (T_{wo} + T_f)/2$ , the Reynolds number Re is based on a uniform velocity profile across the test section and the equivalent diameter is based on that of the subchannels.

Good internal consistency of the data is illustrated in Figure 6 which represents the histogram of the ratio of the experimental HTC to Dittus-Boelter HTC for the complete single-phase heat-transfer data bank. Figure 6 also shows similar results at comparable conditions on a different bundle (same geometry, different heaters) but equipped with mixing vane grids (MVG) every 558 mm. A comparison of the heat transfer coefficient more than 25 cm downstream from the mixing vane grid (where the grid spacer impact on heat transfer is least) shows very similar distribution in HTC ratio compared to the bundle equipped with simple support grids (SSG), and a peak at almost the same HTC ratio of 0.93. Note that, for the same flow and power conditions, local coolant temperatures at the same axial location differ for different types of grids because the mixing vanes improve the subchannel mixing (less enthalpy imbalance). By comparing the HTC ratio for the different test sections, the impact of differences in coolant temperatures has been accounted for by the use of actual coolant temperature data (from the coolant temperature map) in evaluating the experimental HTCs.

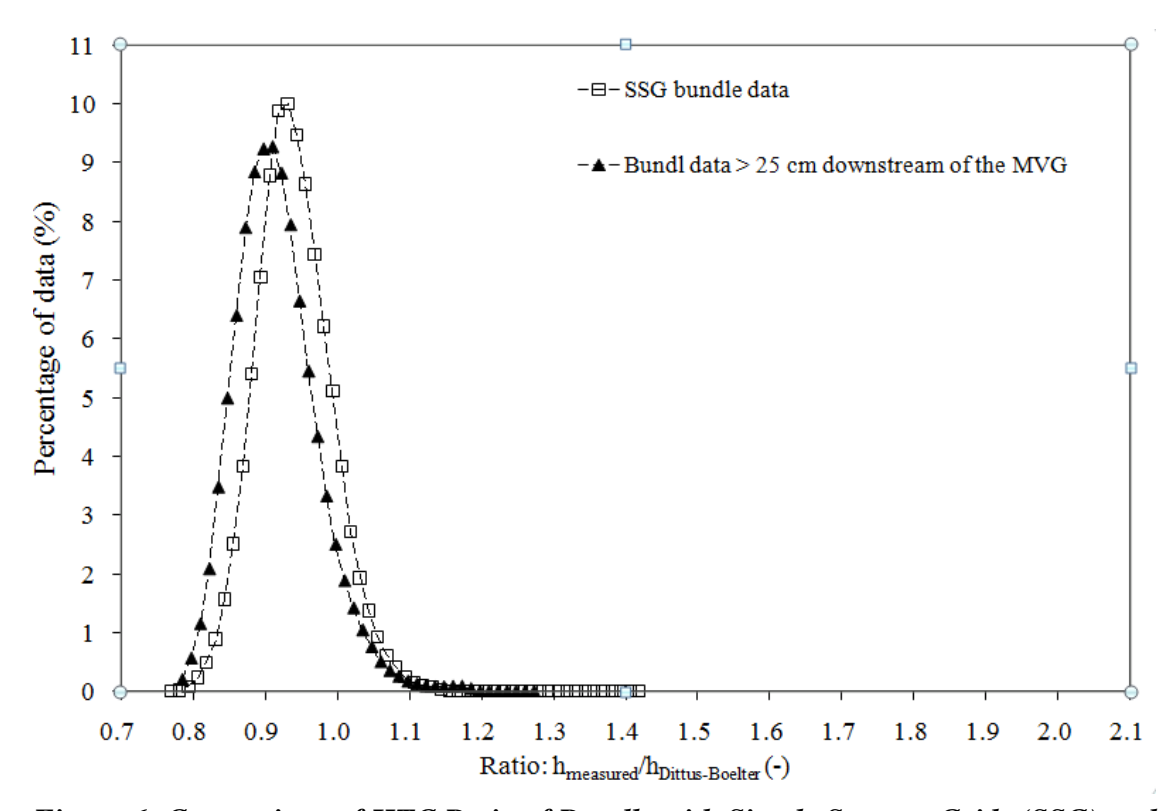


Figure 6: Comparison of HTC Ratio of Bundle with Simple Support Grids (SSG) and Mixing Vane Grids (MVG) for all Rods and all Single Phase Tests.

## 6. BOILING TEST RESULTS

The boiling test results permit a check of the accuracy of outlet temperature measurements and outlet pressure measurements and the fluid temperature measurements. Figure 7 compares the deviation from the saturation temperature *Tsat* (as calculated from outlet pressure measurement of boiling test 4), of the outlet temperature measurement given both by Platinum RTD,

*To-Tsat*, and the average of the 36 subchannel thermocouple measurements, *TFavg-Tsat*. The agreement is very good. The two additional curves present extreme values of the 36 subchannel fluid temperatures i.e. *TFmin-Tsat* and *TFmax-Tsat*. In general the saturation temperature is in excellent agreement with (i) the outlet temperature measured by the platinum RTD (average difference 0.1 K, range 0 to -0.2 K) and (ii) the average of the subchannel outlet-coolant temperature measurements (average difference 0.1 K, range +0.5 to -0.6 K). Further confirmation of the reliability of the wall temperatures, corrected for wall thickness variation comes from a comparison of wall superheats as shown in Figure 8, where a comparison of experimental wall superheat during nucleate boiling and the superheat predicted from the Jens&Lottes equation [4] is shown. Here the experimental wall superheat is obtained as follows:

$$\Delta T_{sat-exp}(Az, z, t) = Two(Az, z, t) - T_{sat}(P_o(t))$$

where:

t is acquisition time,

Az and z are circumferential and axial location respectively,

 $\Delta T_{sat-exp}(Az,z,t)$  is the experimental superheat,

Two(Az,z,t) is outer wall temperature (after correcting for the thickness variation),

 $T_{sat}(P_o(t))$  is the saturation temperature at outlet pressure  $P_o$ .

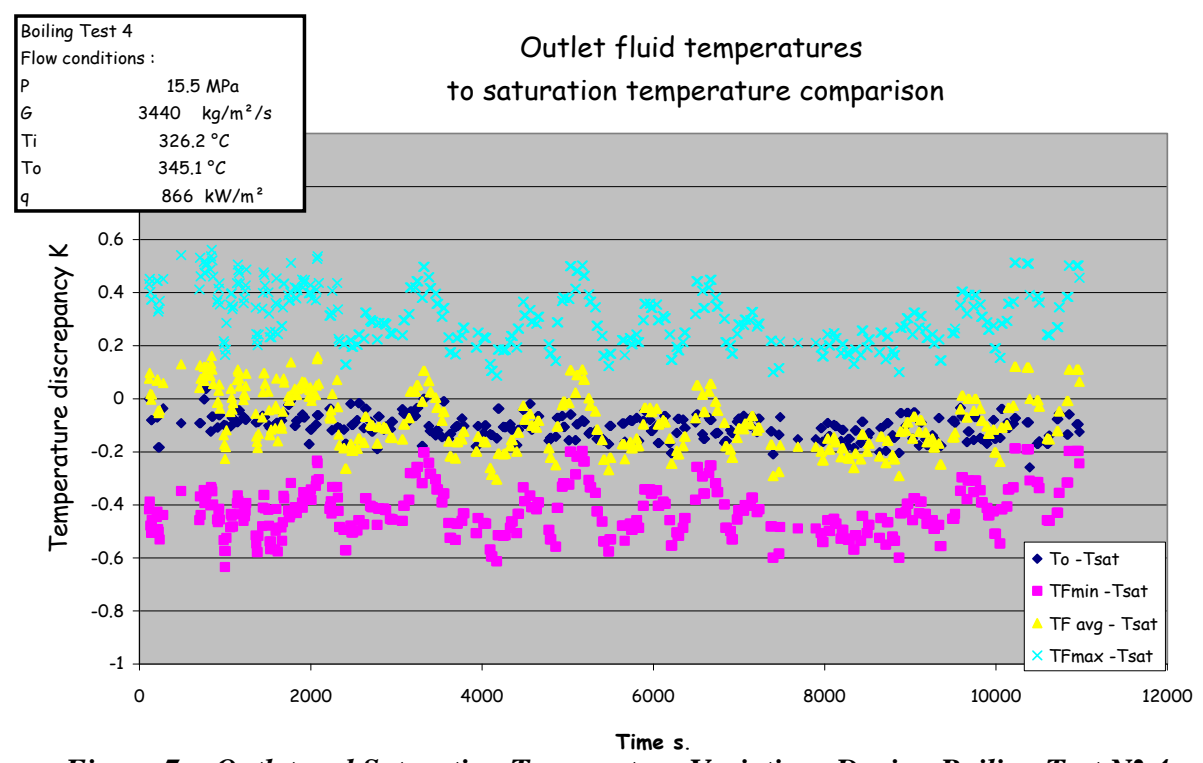


Figure 7: Outlet and Saturation Temperature Variations During Boiling Test N

4.

By correlating the discrepancy of Figure 8 to the axial location one can see that most of the data are within 0.3 K of the regression line. RMS deviation from the regression line is 0.2 K, a value that is comparable to the dispersion observed during calibration process (RMS: 0.1 K) for which no heat flux was applied. The gradient in the discrepancy is partially due to the gradient in saturation temperature due to pressure drop along the length.

#### 7. ONB TEST REPEATABILITY

To assess the repeatability and reliability of the ONB data, two ONB tests were repeated: ONB Run 01-06 once and ONB Run 02-05 twice. Figure 9 presents the maximum spread in coolant temperature (for each available thermocouple) between the ONB tests for each run. The label beside each point identifies the subchannel (numbered 1-36 starting at the bottom left hand side) in which the thermocouple is located. The maximum observed spread is -0.7 K at thermocouple TF19. For ONB Run 01-06 the average spread is -0.2 K (std. dev 0.1 K) and for ONB Run 02-05 it reaches -0.35 K (std. dev 0.1 K). These spreads are similar to those observed during the single-phase heat transfer tests.

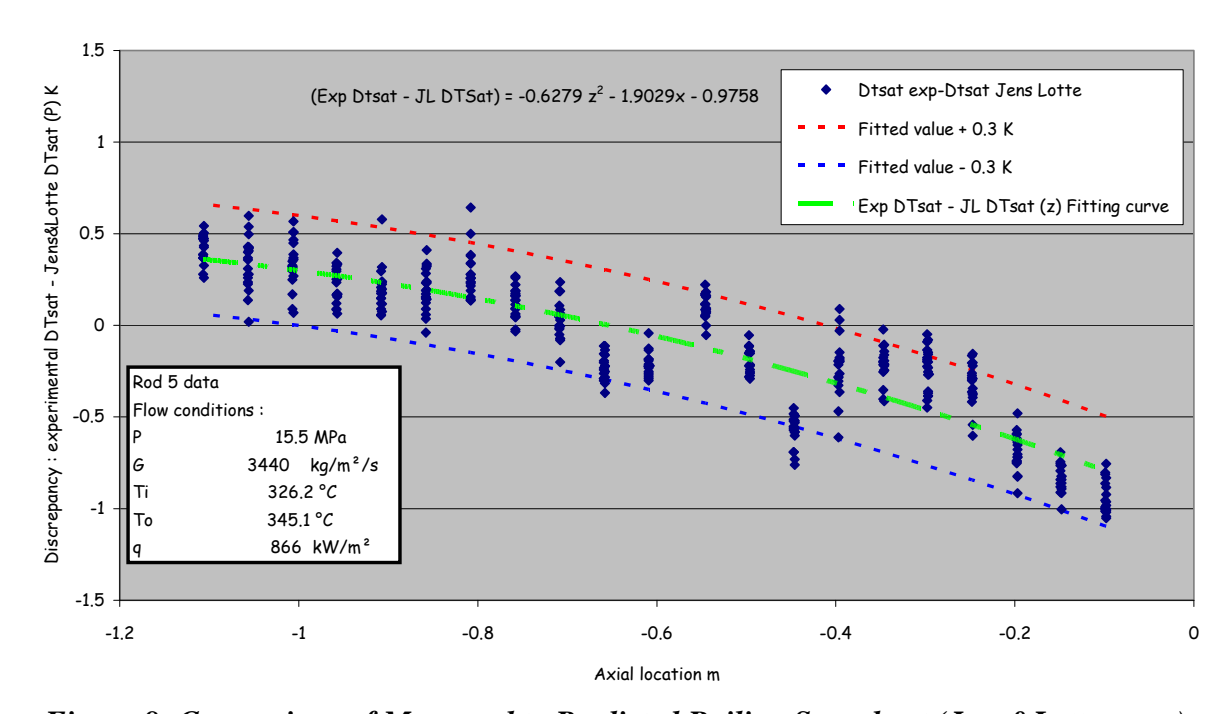


Figure 8: Comparison of Measured to Predicted Boiling Superheat (Jens&Lottes eqn.).

Figure 10 shows an example of the quarter-rod-averaged outer wall temperature of the central rod as a function of cross-sectional-average coolant quality. It is seen that for the central rod, when combining all angles for all repeat runs, the temperatures are within 0.5 K from the average. The same observation applies to the corner rods and side rods. For the same angle the repeatability is even better.

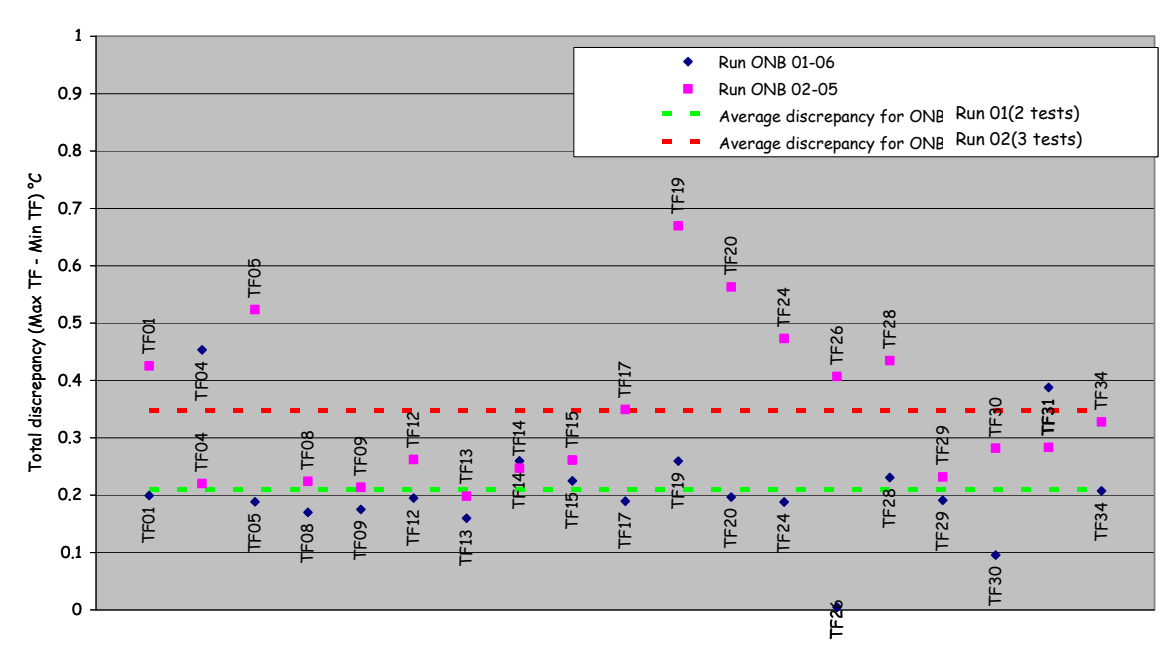


Figure 9: Coolant Temperature Measurement Spreads.

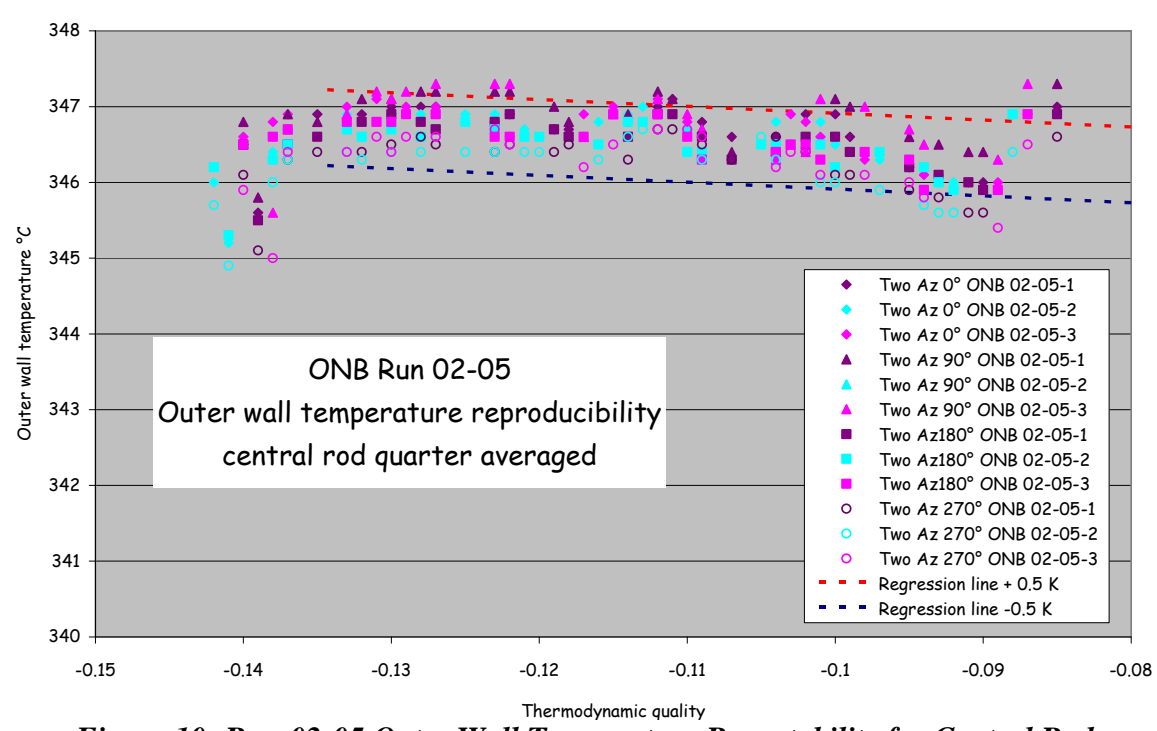


Figure 10: Run 02-05 Outer Wall Temperature Repeatability for Central Rod.

Another approach to checking the repeatability and reliability of the data is by direct comparison between quarter-rod-averaged data for symmetrically-located rods and similar angles. Figure 11 is typical of the whole data bank and presents the results for three side rods (the instrumentation in rod 6 became non-operational during the tests). This figure combines all ONB test results for each run (nominally constant mass flux and heat flux but varying inlet temperature) and each angle, and includes repeat runs. The outer wall temperature vs. thermodynamic quality curve clearly shows two regions. For the lower qualities, the outer wall temperature increases almost linearly with quality, while a "flat" region corresponding to nucleate boiling is reached at the higher qualities.

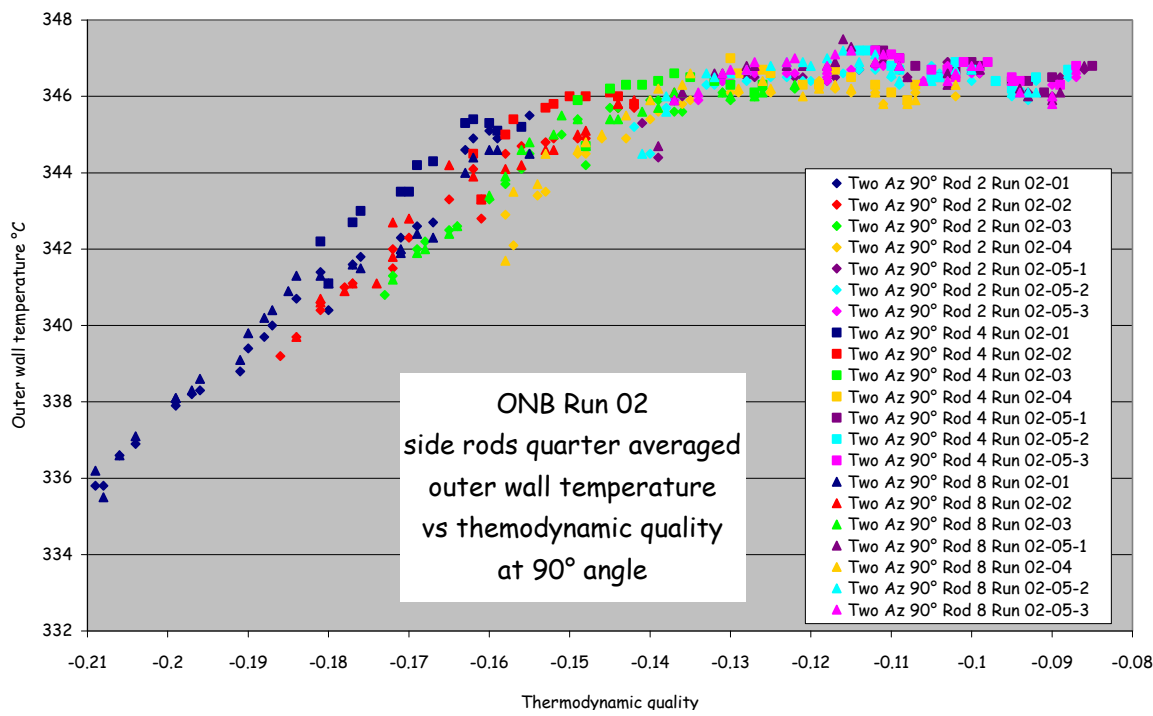


Figure 11: Outer Wall Temperature Comparison of Side Rods for 90° Angle.

Figure 11 shows that the majority of the data are within 1 K from the best-fit line based on all the data. This agreement in wall temperatures is considered excellent since the data include: (i) differences in test conditions between repeat tests (because of small differences in pressure, flow rate, electrical power), (ii) differences in test conditions between runs with different inlet temperatures, (iii) symmetry discrepancies, and (iv) impact of heat transfer enhancement due to the grids. This maximum 1 K variation is typical for the ONB data bank.

When considering all ONB test results, it appears that the ONB quality is independent of inlet temperature: for all tests performed at a constant pressure, heat flux and mass velocity, the ONB for the same symmetric position occurs at the same thermodynamic quality irrespective of location of the nearest low-impact simple support grid. Note that this conclusion is not valid for mixing vane grids that are designed to have a stronger effect on the flow distribution and will therefore likely affect the single phase heat transfer and thus the ONB.

#### 8. CONCLUSIONS

Heat transfer tests were performed in the OMEGA-2 loop to assess the repeatability of bundle heat transfer measurements. The tests were performed on a 5X5 subassembly of a PWR fuel bundle equipped with simple support grids. To extract accurate heat transfer coefficients from bundle heat transfer experiments requires proper experimental procedures i.e. in-situ calibration of all thermocouples, detailed temperature distribution measurements, and correction for variations in tube wall thickness. Three types of tests were performed at PWR conditions of interest: Single Phase Heat Transfer, Onset of Nucleate Boiling tests and the Boiling tests. It was found that as a result of these appropriate experimental procedures:

• generally the difference in heat transfer measurements between repeat runs and between symmetrical locations is very small,

- the agreement between the average subchannel fluid temperature, the outlet temperature and the saturation temperature during the boiling tests is excellent,
- for the boiling tests, the inside wall temperature can be predicted with good accuracy from the Jens&Lottes correlation and the temperature drop across the wall,
- the single phase heat transfer coefficients can be predicted by the Dittus-Boelter correlation corrected by a factor 0.96 for two separate bundles having the same cross sectional geometry

Based on the above observations, it is concluded that the OMEGA-2 loop is capable of obtaining highly accurate and repeatable single phase and boiling heat transfer measurements in PWR-type subassemblies.

#### **NOMENCLATURE**

- Az Angular position
- D<sub>h</sub> Hydraulic diameter
- G Mass velocity
- H Enthalpy
- L Length of the flow meter installation line
- P<sub>o</sub> Pressure
- q Heat flux
- Re Reynolds number
- T Temperature
- $T_f$  Coolant temperature
- $T_i$  Test section inlet temperature
- $T_o$  Test section outlet temperature
- *Tsat* Saturation temperature
- W Test section power
- z Axial distance measured from the end of the heated length
- $\varphi$  Heat flux or angular position

## **ACRONYMS**

CHF Critical Heat Flux
EOHL End Of Heated Length
HTC Heat Transfer Coefficient

ID Inside Diameter
NB Nucleate Boiling
OD Outside Diameter

ONB Onset of Nucleate Boiling

RTD Resistance Temperature Detector

## **REFERENCES**

- [1] Cubizolles, G. et al., 2009a, PWR Bundle Heat Transfer Tests In The OMEGA-2 Test Facility, Proceedings, NURETH-13 Conference, Kazanawa, Japan 2009.
- [2] Cubizolles, G. et al., 2009b, Methods for Determining the Wall Thickness Variation of Tubular Heaters Used in Thermalhydraulic Studies, PWR Bundle Heat Transfer Tests In

- The OMEGA-2 Test Facility, Proceedings, NURETH-13 Conference, Kazanawa, Japan 2009.
- [3] Dittus, F.W. and Boelter, L.M.K., 1930, Heat Transfer in Automobile Radiators of the Tubular Type, University of California Publications, Vol. 2, 443-461.
- [4] Jens, W.H. and Lottes, P.A., 1951, Analysis of Heat Transfer Burnout, Pressure Drop and Density Data for High Pressure Water, USAEC report ANL-4627.
- [5] Leung, L.K.H., Pioro, I.L. and Bullock, D.E., 2003, Post dryout surface temperature distributions in a vertical Freon cooled 37 rod bundle, Proceedings, 10<sup>th</sup> International Topical meeting on Nuclear Reactor Thermal-hydraulics, Seoul, Korea, October 5-9.
- [6] Schenk, J.R. and D.C. Groeneveld, D.C., 1990, Measurement of Thermalhydraulic Parameters Inside Multi-Element Bundles, Proceedings, International Symposium on Multi-Phase Flow, Miami, Dec 9-12.
- [7] New Experimental Studies of Thermal-Hydraulics of Rod Bundles (NESTOR), Project Overview and Feasibility Studies, EPRI, Palo Alto, CA, EDF, France, and CEA, France: 2005. Report No. 1011089.
- [8] Standard NF EN 60584-2: "Thermoelectric couples Second part (tolerances)". July 1993.
- [9] Standard NF EN 60584-1: "Thermoelectric couples First part (reference tables)". February 1996.